Int J Thermophys (2008) 29:2136–2148
DOI 10.1007/s10765-008-0483-0

Spectral Reflectance of the Close-Packed Structure of Silica Microspheres

Masahiro Kihara · Koji Miyazaki · Hiroshi Tsukamoto

Published online: 17 July 2008

Abstract The spectral reflectance of microperiodic structures of silica microspheres was investigated. The electromagnetic dispersion relation in a close-packed structure of silica spheres is computed. The three-dimensional close-packed structures, self-assembled with silica microspheres (2 μm and 3 μm), were rapidly fabricated over a large area. Specular reflectance was measured by using Fourier transform-infrared spectroscopy (FT-IR). The experimental results were evaluated by a modification of Bragg's law, taking into account Snell's law of refraction, and calculations of multiple reflections and the scalar wave approximation method. In addition, to expand the reflection wavelength range, a double-layered sample was fabricated, and its spectral reflectance was determined.

Keywords Close-packed structure · FT-IR · Microperiodic structures · Self-assembly · Silica microspheres

1 Introduction

Thermal radiation is energy transferred by electromagnetic waves. Thermal radiative properties of materials can be improved artificially by microstructured surfaces [1–4]. The propagation of electromagnetic waves can be controlled by microperiodic structures such as photonic crystals [5,6]. Photonic crystals can form a frequency bandgap for electromagnetic radiation much like natural crystals having a bandgap for electrons. Incident electromagnetic radiation is reflected by photonic crystals because propagation of electromagnetic waves is inhibited at a photonic gap [7,8]. Hence,

M. Kihara · K. Miyazaki (✉) · H. Tsukamoto
Department of Biological Functions and Engineering, Kyushu Institute of Technology,
2–4 Hibikino, Wakamatsu-ku, Kitakyushu, Fukuoka 808-0196, Japan
e-mail: miyazaki@life.kyutech.ac.jp

photonic crystals are expected to be used for a thermal radiation shield [9,10], i.e., suppression of thermal radiation [11].

However, fabricated photonic crystals have been very small for thermal engineering applications because standard microfabrication processes are used for sample preparation. Large photonic crystals are fabricated by means of colloidal techniques to solve the size issue. The prepared large photonic crystals are called colloidal photonic crystals [12–14]. Macroscopic periodic dielectric spheres induce Bragg diffraction for incident electromagnetic waves at specific wavelengths. Optical properties of colloidal crystals assembled with dielectric submicron spheres have been studied experimentally and theoretically [15–17]. The colloidal crystals can be applied to modify thermal radiative properties by increasing the size of particles. It is one of the problems that the reflection wavelength range of colloidal crystals assembled with only one size of dielectric spheres is too narrow for thermal radiation reflection. To solve this issue, a multilayer colloidal crystal may be useful to expand the reflection wavelength range [18].

In this paper, the spectral reflectance of microperiodic structures of silica microspheres of well-defined thickness are investigated in the infrared region. The electromagnetic dispersion relation in a close-packed structure of silica spheres is computed, and then the sizes of particles are determined to reflect the infrared range. The samples are fabricated over a Si substrate by layer-by-layer stacking of hexagonally close-packed monolayers of silica microspheres. The sample configurations are observed by a scanning ion microscope (SIM). The spectral reflectances of microperiodic structures are measured using a microscopic FT-IR spectrometer. The measured spectral reflectances are evaluated by using a modification of Bragg's law, taking into account Snell's law of refraction, and calculations of multiple reflections (MRs) and the SWA.

2 Microperiodic Structure Design

Microperiodic structures were designed by using a numerical code named MIT Photonic Band (MPB) [19]. The dispersion relation of electromagnetic waves in an face-centered-cubic (fcc) lattice of dielectric spheres was computed by MPB. In this study, prepared samples are close-packed structures of silica microspheres fabricated by self-assembly. The close-packed structure takes three possible stacking structures: *ABC* type as fcc lattice, *ABA* type as hexagonal-close-packed (hcp) structure, and a mixture of fcc and hcp. From experimental observations, fcc is more stable than hcp [15,20]. Therefore, an fcc lattice was considered as a periodic structure in the calculation. In this calculation, the dimensionless radius, r/a, and the dielectric constant of spheres, ε, can be used as parameters. The dimensionless radius $r/a = 0.354$ because of the close-packed structure of spheres. The dielectric constant, ε, can be expressed as $\varepsilon\varepsilon' + i\varepsilon'' = n^2 - k^2 + i2nk$. The refractive index of silica, n_{silica}, is approximately 1.4, and the extinction coefficient, k_{silica}, is from 10^{-2} to 10^{-5} [21] in the infrared range, especially below 8 μm in wavelength. Thus, the dielectric constant of silica, $\varepsilon_{\text{silica}}$, is calculated to be 1.96. The computed dispersion relation of electromagnetic waves is shown in Fig. 1. The solid and broken lines show the computed transverse magnetic (TM) and transverse electric (TE) bands against the special k-points labeled

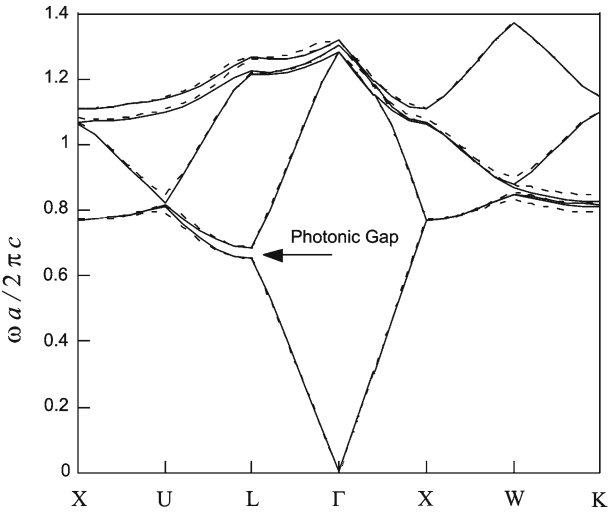

Fig. 1 Photonic band structure of fcc lattice of dielectric spheres

in the Brillouin zone. The Γ-L direction corresponds to the [111] direction in an fcc lattice. The photonic gap appeared at $\omega a/(2\pi c) = 0.67$ in the Γ-L direction. The numerical results show that the relation between the photonic gap wavelength, λ, and the center-to-center distance, D, of a close-packed structure is expressed by

$$\lambda = a/0.67 = \sqrt{2}D/0.67 = 2.11D \tag{1}$$

where D is equal to the particle diameter, d, because of the close-packed structure. According to results of the numerical analysis, the sizes of the silica spheres were selected as 2 μm and 3 μm in diameter to enhance reflectance in the infrared range.

3 Fabrication of Microperiodic Structure

Mono-dispersed silica microspheres (2 μm and 3 μm in diameter) were obtained from Catalysts & Chemicals Ind. Co, Ltd. A few drops of a suspension of silica microspheres were dropped onto a water surface by using a microsyringe. The silica microspheres form a hexagonally close-packed monolayer by self-assembly as the solvent evaporates over the water surface. The mechanism of two-dimensional crystallization is governed by the capillary forces between particles partially protruded from a solvent surface, and the crystal grows through convective particle flux caused by the solvent evaporation from the already ordered array [22]. After the solvent evaporates completely, the monolayer of silica microspheres was transferred to a Si substrate [23]. The size of the Si wafer is up to 5 cm (2 in) with a double-sided mirror surface and a thickness of 0.3 mm. The sample was dried on a hot plate. The thickness of the samples was controlled precisely by repeating these processes. We prepared samples consisting of 3, 5, 8, and 10 layers of close-packed silica microspheres (2 μm and 3 μm in

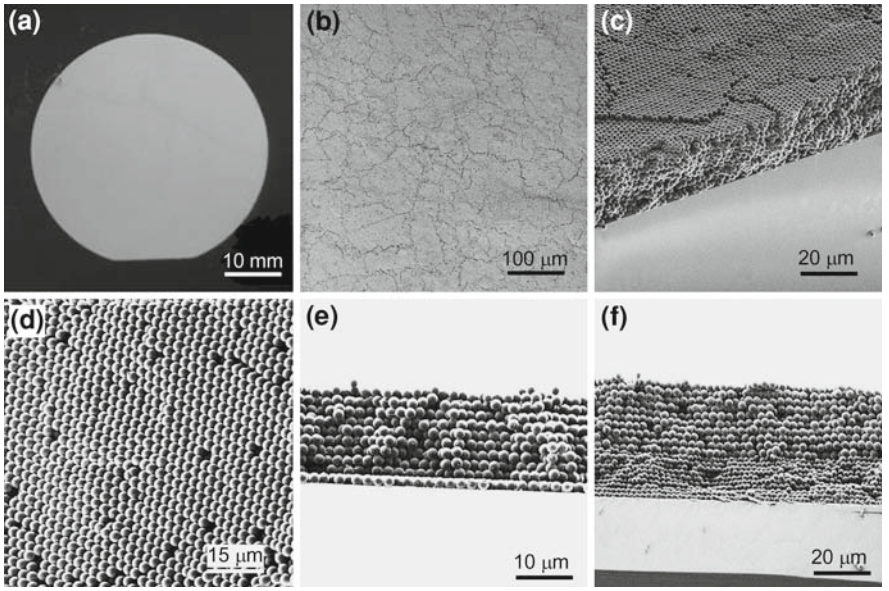

Fig. 2 Sample images: (**a**) full images, (**b**) surface, (**c**) oblique, (**d**) particle arrays, (**e**) cross-sectional image of a 10-layered sample, and (**f**) cross-sectional image of a double-layered close-packed structure

diameter). In addition, a double-layered sample which had 10 layers of close-packed 3 μm silica spheres on 10 layers of close-packed 2 μm silica spheres was prepared.

4 Observation of Sample Configuration

The fabricated samples were observed by mean of SIM (JFIB-2300, Seiko Instruments Inc.), as shown in Fig. 2. Although dislocations and lattice defects were observed, the silica microspheres formed a close-packed structure over a large area. The diameters of the silica spheres were measured directly from the SIM images by using image analysis software (Asahi Kasei Engineering). The measured average diameters of 2 μm and 3 μm samples were 2.07 μm and 2.82 μm, respectively.

5 Measurements of Spectral Reflectance

The spectral reflectance was measured by using a microscopic FT-IR spectrometer (Micro FT/IR-300, JASCO). The focal point was adjusted to the surface of a sample. The incident light enters the surface of a sample with an incident angle of 20° through a Cassegrain mirror, and then specularly reflected light is collected by the same Cassegrain mirror and fed to a detector (mercury cadmium telluride, MCT). The transmitted light passes through to the back of a sample, and does not contribute to the measurement. The measuring infrared wavelength range is from 2.5 μm to

15.4 μm (from 650 cm^{-1} to 4000 cm^{-1}). The measuring area of the sample surface is 300 μm × 300 μm.

The reflectance of the real surface consists of mostly a specular component and a diffuse component. However, we focused only on the specular component, because the effects of microperiodic structures strongly appear in the specular component.

The reflection spectrum of a gold mirror was measured as a reference $I_0(\lambda)$ prior to the following measurements. Next the reflection spectrum of a sample $I_r(\lambda)$ was measured. The spectral reflectance of a sample $\rho(\lambda)$ is calculated as the ratio of the measured result of a sample to that of a reference per the following equation:

$$\rho(\lambda) = I_r(\lambda)/I_0(\lambda). \tag{2}$$

6 Optical Properties of Close-Packed Silica Microspheres

6.1 Bragg's Law

The approximate prediction of the reflection peak wavelength, λ, due to Bragg diffraction from colloidal crystals have been expressed by a modification of Bragg's law, taking into account Snell's law of refraction [12,13,17], for an arbitrary incident angle, θ,

$$\lambda = 2d_{111}\sqrt{n_{\text{eff}}^2 - \sin^2\theta}. \tag{3}$$

where d_{111} is the interplanar spacing of (111) planes of a close-packed structure, and is given by $d_{111} = \sqrt{2/3}D$. The effective refractive index, n_{eff}, is expressed as [12,13,24,25]

$$n_{\text{eff}}^2 = \phi n_{\text{SiO}_2}^2 + (1-\phi)\, n_{\text{air}}^2. \tag{4}$$

where n_{silica} and n_{air} are refractive indexes of silica and air. The refractive index of silica in the infrared range from 2 μm to 7.5 μm in wavelength [21] is approximately 1.4, while the value for n_{air} is 1.0. ϕ is the volume fraction of the spheres. Thus, n_{eff} is calculated to be 1.31.

6.2 Scalar Wave Approximation

The quantitative prediction of the optical properties of the colloidal crystals based on the SWA has been performed [26]. The peak wavelength and width of the reflection peak due to Bragg diffraction as a function of the numbers of layers are described by the SWA. The solution of the Maxwell equation for an electric field in a periodic structure leads to expressions for the transmission rate T_{SWA},

$$T_{\text{SWA}} = \frac{2\beta_0 \exp(-ik_0 N d_{111})}{2\beta_0 \cos(kNd_{111}) - i\left(1+\beta_0^2\right)\sin(kNd_{111})}. \tag{5}$$

where N is the number of layers. k_0, k, and β_0 are analytical expressions depending on other parameters not described here (For details, see Ref. [26]). If we neglect absorption, the reflection rate R_{SWA} can be expressed as $R_{\mathrm{SWA}} = 1 - T_{\mathrm{SWA}}$.

At wavelengths greater than 7.5 μm, the refractive index and extinction coefficient of silica become too large; thus, the reflection rate is not accurately calculated. Therefore, the reflection rate at wavelengths smaller than 7.5 μm is adopted here. The optical constants of silica as a function of wavelength [21] are used in this calculation.

6.3 Multiple Reflections

The difference between the refractive index of the layer of close-packed silica microspheres and the Si substrate may cause MRs inside each medium. If we assume the layer of close-packed silica microspheres is a homogeneous plane sheet with an effective refractive index, n_{eff}, and an effective extinction coefficient, k_{eff}, the radiative properties of the plane sheet is determined through geometric optics and ray tracing [27]. The reflection coefficient, taking into account multiple reflections inside the plane sheet and substrate can be approximately expressed as

$$R_{\mathrm{MRs}} = r_{12} + \frac{r_{23}\,(1 - r_{12})^2\,\tau_2^2}{1 - r_{12} r_{23} \tau_2^2} + \frac{r_{34}\,(1 - r_{12})^2\,(1 - r_{23})^2\,\tau_2^2 \tau_3^2}{1 - r_{23} r_{34} \tau_3^2}. \tag{6}$$

where r_{ij} is the reflectance at the interfaces between two contiguous media. In this calculation, the incident angle is the normal incidence, although the incident angle is 20° in this experiment because of a small discrepancy from Fresnel's equations. For the case of normal incidence, the reflectance at the interface [27] is

$$r_{ij} = \frac{\left(n_j - n_i\right)^2 + k_j^2}{\left(n_j + n_i\right)^2 + k_j^2}. \tag{7}$$

The optical constants of silica as a function of wavelength [21] are used in this calculation. τ is the transmittance of the medium, and is expressed as

$$\tau = \exp[-4\pi k h/\lambda_0]\,. \tag{8}$$

where k is the extinction coefficient, and λ_0 is the wavelength of incident radiation. h is the thickness, and the thickness of the sample h_{smp} consisting of N layers of particle diameter, d, can be calculated as

$$h_{\mathrm{smp}} = [(N - 1)\,d_{111} + 1]\,d. \tag{9}$$

7 Results and Discussion

The experimental spectral reflectances of samples which consist of close-packed silica microspheres (2 μm and 3 μm in diameter) made up of 3, 5, 8, and 10 layers are shown in

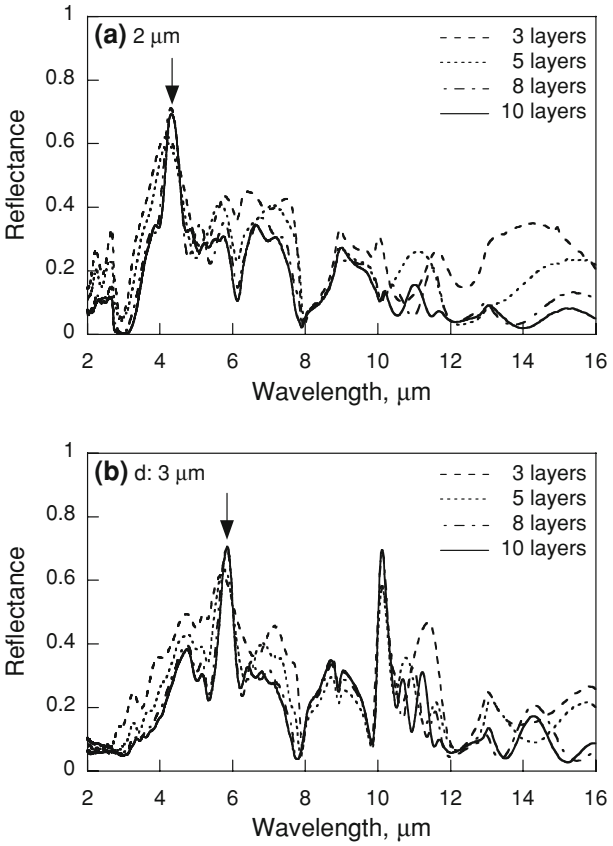

Fig. 3 Spectral reflectance of samples consisting of silica microspheres: (**a**) 2 μm silica spheres and (**b**) 3 μm silica spheres

Fig. 3. The reflection peak due to Bragg diffraction appeared at a specific wavelength depending on the particle size. The (arrowed) reflection peak becomes higher and narrower with an increasing number of layers, and the peak position shifts to longer wavelengths. The peak wavelengths are 4.32 μm and 5.90 μm for samples consisting of 10 layers of 2 μm and 3 μm silica spheres, respectively. A broad reflection increase under the Bragg reflection peak is observed in the wavelength range below 8 μm, and it decreases with an increase in the number of layers.

The reflection peak wavelength due to Bragg diffraction as a function of the incident angle is approximately expressed by a modification of Bragg's law, taking into account Snell's law of refraction. Comparisons between the experimental and calculated reflection peak wavelengths are shown in Fig. 4. The calculated peak wavelengths are 4.27 μm and 5.81 μm for samples of close-packed, 2 μm and 3 μm, silica spheres, respectively. The experimental values are well reproduced by the equation.

The experimental reflection spectrum of close-packed silica microspheres fabricated over a Si substrate includes mainly Bragg diffraction, multiple reflections, and

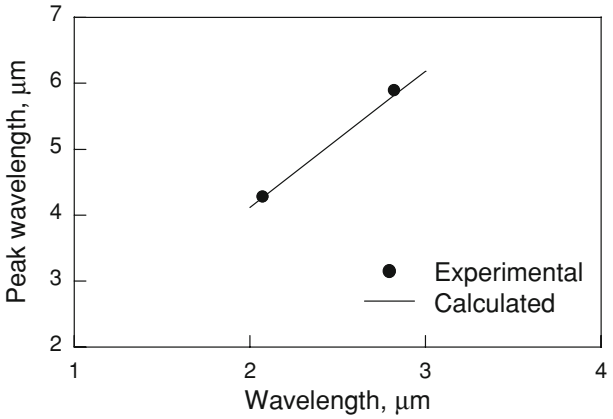

Fig. 4 Peak wavelength of spectral reflectance of samples with different diameters of silica spheres

solid-state properties of silica. To understand the experimental spectra, we consider these effects separately. The spectral reflectances calculated by Eqs. 5 and 6 for samples which consist of close-packed silica microspheres (2 μm and 3 μm in diameter) made up of 3, 5, 8, and 10 layers are shown in Fig. 5.

From SWA calculations, the Bragg reflection peak position and peak width vary with an increase in the number of layers. Comparisons between the experimental and calculated Bragg reflection peak wavelengths and peak widths as a function of the thickness of the samples (the number of layers) is shown in Fig. 6. The plotted values are normalized by the Bragg wavelength, λ_B, calculated by SWA. The Bragg reflection peak wavelength converges to the Bragg wavelength by increasing the number of layers sufficiently (more than about 50 layers). The reflection peak shifts slightly to longer wavelengths with an increase in the number of layers in the experiment. On the contrary, the reflection peak shifts to shorter wavelengths in the calculation of the SWA. Although the shifting direction is reversed, both reflection peaks approach asymptotically to the Bragg reflection peak wavelength. The experimental data of samples of 3 μm silica spheres slightly overlap. The optical constant of silica spheres may not agree with the reference value. The magnitudes of reflectances between experimental and calculated results are not consistent. The peak width become narrower with an increase in the number of layers, and becomes consistent for the sample consisting of 10 layers.

From the calculation of the reflectance considering multiple reflections, the reflectance increases at wavelengths <8 μm, and the magnitude of the reflectance decreases with an increase in the number of layers, as in the experiment. Comparisons between experimental and calculated reflectances for close-packed silica microspheres (2 μm and 3 μm in diameter) consisting of 10 layers are shown in Fig. 7. The magnitude of the reflectance is of the same order for both experimental and calculated reflectances.

In the wavelength range from 8 μm to 12 μm, the strong reflection peak is due to the solid-state properties of silica. Although the magnitude is not consistent, the peak position is the same, so that this reflection peak is identified as a solid-state property

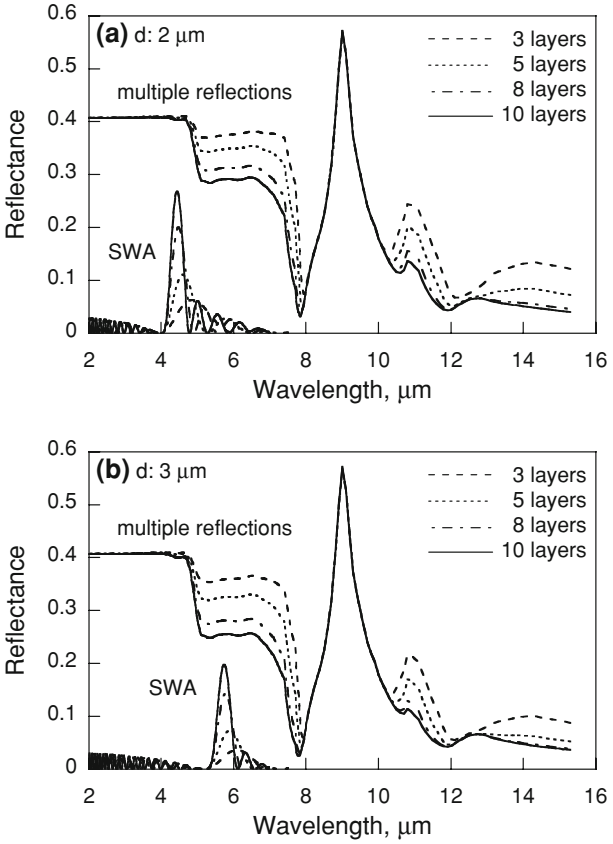

Fig. 5 Calculated reflectance of multiple reflection and SWA calculation: (**a**) 2 μm silica spheres and (**b**) 3 μm silica spheres

of silica. At wavelengths below 5 μm, the reflectance is constant with a value of approximately 0.4 in the calculation of multiple reflections.

This is not consistent within experimental results. The propagating light is scattered by particles, and the specular component decreases. The reason for the strong peak of reflection of 3 μm samples at 10.5 μm wavelength is unknown. It is possibly due to some kind of substance added by the manufacturer.

The reflection wavelength range of a close-packed structure which consists of only one size of silica particles is too narrow. The multiple wavelength range can be reflected by stacking layers consisting of different size particles [14,16]. To enhance the reflectance at multiple wavelengths, a double-layered sample, stacking 10 layers of 3 μm silica spheres on 10 layers of 2 μm silica spheres, was fabricated. The measured spectral reflectance is shown in Fig. 8. Two reflection peaks appeared simultaneously at 4.29 μm and 5.80 μm. The two peaks correspond to reflection peaks of samples consisting of 2 μm and 3 μm silica spheres. Therefore, the double-layered sample combines the properties of each layer. However, the reflectance at each peak of the double-lay-

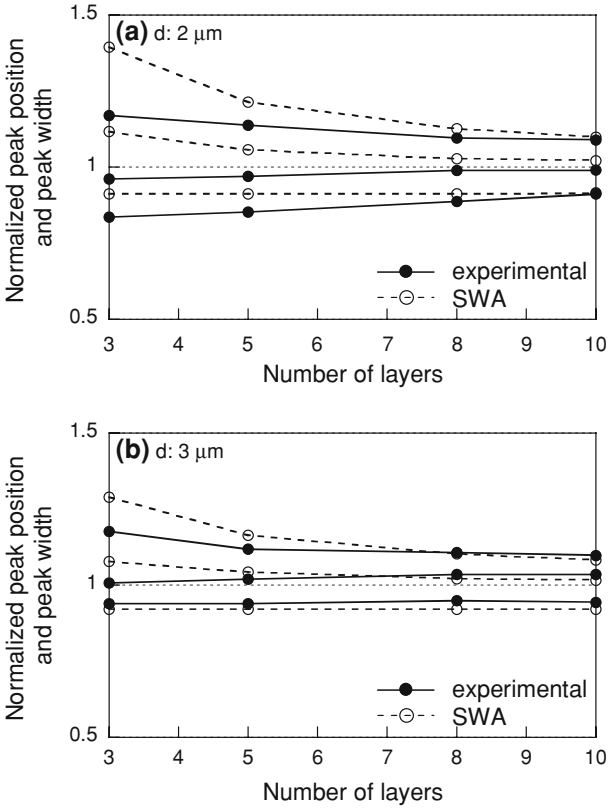

Fig. 6 Variation of reflection peak position and width as the function of the number of layers: (**a**) 2 μm silica spheres and (**b**) 3 μm silica spheres

ered sample is lower than the reflectances of samples consisting of only one size of silica spheres. A stacking structure for which the reflectance becomes a maximum with a broad reflection wavelength range is required.

8 Summary

The spectral reflectance of close-packed silica microspheres is investigated in the infrared wavelength range. The electromagnetic dispersion relation in a close-packed structure of spheres is computed. The photonic gap is found at a frequency $\omega a/(2\pi c) = 0.67$. The close-packed structures are prepared over a large area by self-assembly with silica microspheres; particle sizes are 2 μm and 3 μm to enhance the reflectance in the infrared range. Close-packed structures which assembled with only one size of silica spheres and a double-layered close-packed structure which formed by layer-by-layer stacking are fabricated with silica microspheres on a Si substrate. The spectral reflectances are measured by using an FT-IR spectrometer. The reflection peak due to Bragg diffraction appears at a specific wavelength depending on particle size. The

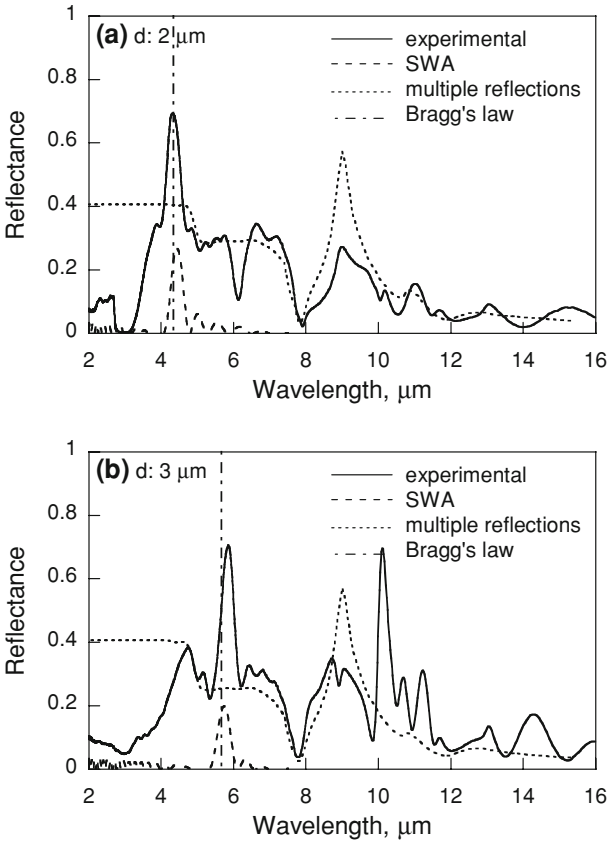

Fig. 7 Comparison between experimental and calculated spectral reflectance of 10-layered sample: (**a**) 2 μm silica spheres and (**b**) 3 μm silica spheres

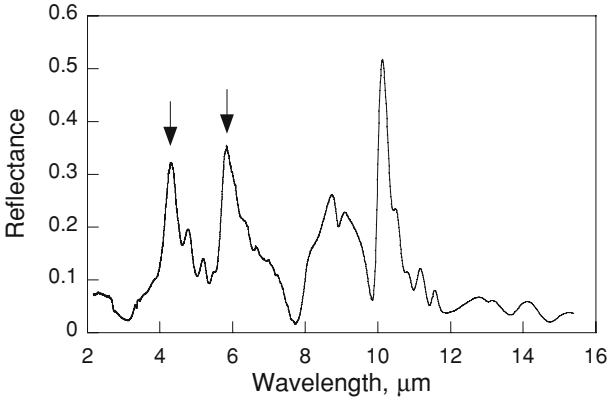

Fig. 8 Spectral reflectance of a double-layered close-packed structure

reflection peak position shifts asymptotically to the Bragg wavelength, and the peak width become narrower with an increase in the number of layers. The reflection peak wavelengths on samples consisting of 10 layers are 4.29 μm and 5.90 μm on samples of 2 μm and 3 μm silica spheres, respectively. The peak wavelengths correspond to Bragg's law, taking into account Snell's law of refraction. From calculation of the reflectance considering multiple reflections inside a sample and substrate, the magnitude of the reflectance is of the same order at wavelengths greater than the Bragg wavelength. The variation of peak position and width with an increase in the number of layers is explained by the comparison between experimental and SWA calculated results. Although the direction of peak shifts is opposite, the peak shifts asymptotically to the Bragg wavelength. The peak width narrows with an increase in the number of layers, and becomes consistent for the sample consisting of 10 layers. The magnitude of the reflection peak is not consistent. In the reflection spectrum of double-layered close-packed structure, two reflection peaks appeared simultaneously. The two peaks can be explained by the reflection spectrum of each layer.

Acknowledgments The authors thank Prof. Gang Chen of Massachusetts Institute of Technology, Profs. Toshiro Makino and Hidenobu Wakabayashi of Kyoto University, Prof. Katsunori Hanamura of Tokyo Institute of Technology, and Prof. Jun Yamada of Shibaura Institute of Technology for helpful discussions. K. Miyazaki gratefully acknowledges the support by JSPS under Grant No. 14655086, Tanikawa foundation, and Hosokawa Powder Technology Foundation.

References

1. P.J. Hesketh, B. Gebhart, J.N. Zemel, Trans. ASME J. Heat Transfer **110**, 680 (1988)
2. J.L. Gall, M. Olivier, J.-J. Greffet, Phys. Rev. B **55**, 10105 (1997)
3. J.-J. Greffet, R. Carminati, K. Joulain, J.-P. Mulet, S. Mainguy, Y. Chen, Nature **416**, 61 (2002)
4. S. Maruyama, T. Kashiwa, H. Yugami, M. Esashi, Appl. Phys. Lett. **79**, 1393 (2001)
5. E. Yablonovitch, Phys. Rev. Lett. **58**, 2059 (1987)
6. J.D. Joannopolous, R.D. Meade, J.N. Winn, *Photonic Crystals* (Princeton University Press, Princeton, 1995)
7. J.G. Fleming, S.Y. Lin, I. Dl-Kady, R. Biswas, K.M. Ho, Nature **417**, 52 (2002)
8. S.Y. Lin, J. Moreno, J.G. Fleming, Appl. Phys. Lett. **83**, 380 (2003)
9. K. Matsumura, T. Naganuma, Y. Kagawa, Adv. Eng. Mater. **5**, 226 (2003)
10. T. Naganuma, Y. Kagawa, Acta Mater. **52**, 5645 (2004)
11. F. Kusunoki, H. Kawabata, T. Hiroshima, J. Takahara, T. Kobayashi, T. Sumida, S. Yanagida, Electron. Lett. **39**, 622 (2003)
12. S.-L. Kuai, X.-F. Hu, A. Hache, V.-V. Truong, J. Cryst. Growth **267**, 317 (2004)
13. H. Fudouzi, J. Colloid Interface Sci. **275**, 277 (2004)
14. S. Reculusa, P. Masse, S. Ravaine, J. Colloid Interface Sci. **279**, 471 (2004)
15. P.N. Pusey, W. van Megen, P. Bartlett, B.J. Ackerson, J.G. Rarity, S.M. Underwood, Phys. Rev. Lett. **63**, 2753 (1989).
16. P. Jiang, J.F. Bertone, K.S. Hwang, V.L. Colvin, Chem. Mater. **11**, 2132 (1999)
17. S.G. Romanov, T. Maka, C.M. Sotomayor Torres, M. Muller, R. Zentel, D. Cassagne, J. Manzanares-Martinez, C. Jouanin, Phys. Rev. E **63**, 065503 (2001)
18. P. Jiang, G.N. Ostojic, R. Narat, D.M. Mittleman, V.L. Colvin, Adv. Mater. **13**, 389 (2001)
19. S.G. Johnson, J.D. Joannopoulos. Available from: http://ab-initio.mit.edu/mpb. Accessed July 2005 (1999)
20. C. Dux, H. Versmold, Phys. Rev. Lett. **78**, 1811 (1997)
21. E.D. Palik, G.Ghosh, *Handbook of Optical Constants of Solids* (Academic Press, New York, 1985), pp. 747–763

22. N.D. Denkov, O.D. Velev, P.A. Kralchevsky, I.B. Ivanov, H. Yoshimura,K. Nagayama, Nature **361**, 26 (1993)
23. Y. Ohkura, H. Harada, A. Shimizu, K. Watanabe, A. Nakashima, K. Inoue,K. Ohno, M. Teramoto, M. Komatsu, in *Proceedings VMIC Conf.* (1993), pp. 233–239
24. E. Mine, M. Hirose, D. Nagao, Y. Kobayashi, M. Konno, J. Colloid Interface Sci. **291**, 162 (2005)
25. D.A.B. Filho, C. Hisano, R. Bertholdo, M.G. Schiavetto, C. Santilli, S.J.L. Ribeiro, Y. Messaddeq, J. Colloid Interface Sci. **291**, 448 (2005)
26. D.M. Mittleman, J.F. Bertone, P. Jiang, K.S. Hwang, V.L. Colvin, J. Chem. Phys. **111**, 345 (1999)
27. M.Q. Brewster, *Thermal Radiative Transfer and Properties* (Wiley, New York, 1992)